The Influence of Plasma Glucose Levels on Fluorine-18-Fluorodeoxyglucose Uptake in Bronchial Carcinomas

K.-J. Langen, U. Braun, E. Rota Kops, H. Herzog, T. Kuwert, B. Nebeling and L.E. Feinendegen

Institute of Medicine and Institute of Nuclear Chemistry, Research Center, Jülich, Germany

PET studies with 2-^{18}F-fluorodeoxyglucose (FDG) were carried out in 15 patients with bronchial carcinomas, first under fasting conditions and then 2 days later during intravenous infusion of a 20% glucose solution which raised the plasma glucose level from 84.6 ± 14.7 to 168.3 ± 23.6 mg/100 ml ($n = 15$, $p < 0.001$). Tumor metabolism was quantified by the dose absorption ratio (DAR) of FDG uptake [DAR = tissue concentration/(injected dose/body weight)] and also by the rate of glucose consumption (MR) as measured by the Patlak graphical approach in 12 patients. The DAR decreased from 5.07 ± 1.89 under fasting conditions to 2.84 ± 0.97 (−41.8% ± 15%, $n = 15$, $p < 0.001$) during glucose infusion, while the MR remained constant (4.71 ± 2.38 mg/100 ml/min versus 4.96 ± 2.46 mg/100 ml/min, $n = 12$, ns). Correction of the DAR data by plasma glucose level eliminated the significant difference between the fasting and glucose load [4.24 ± 1.59 versus 4.70 ± 1.45 ($n = 15$, ns)], but considerable changes in individual patients remained. These data indicate that the DAR of FDG uptake in bronchial carcinomas is influenced significantly by plasma glucose levels. Dynamic quantification of glucose metabolism using the Patlak approach is less dependent on the plasma glucose level and appears advantageous when high reproducibility is needed.

J Nucl Med 1993; 34:355–359

The potential value of measuring glucose metabolism for tumor diagnosis and assessing the progress of therapy has been recognized since the early days of positron emission tomography (PET) (*1*). This recognition is based on the observation that many rapidly growing tumor cells exhibit increased glycolysis (*2*). During the last decade, many studies of glucose metabolism in human tumors have been performed using 2-^{18}F-fluorodeoxyglucose (FDG) and PET, suggesting great promise for future clinical applications (*3*). The majority of PET FDG tumor studies, other than those of brain tumors, have been based on nonkinetic evaluations of tumor FDG uptake, compared either to normal tissue or to injected dose per body weight (*4*). The latter is referred to as the dose absorption ratio (DAR), differential uptake ratio (DUR) or standardized uptake value (SUV). The reliability of this approach has been investigated insufficiently, especially with respect to the influence of plasma glucose levels in various types of tumors. The present study assesses the influence of the plasma glucose level on the DAR of FDG uptake in bronchial carcinomas. For comparison, an approach to quantify glucose metabolism in absolute terms was also considered.

MATERIAL AND METHODS

Fifteen patients with bronchial carcinomas, 12 males and 3 females with a mean age 60 ± 11 yr, were studied using PET and FDG. Ten of the patients had squamous-cell carcinomas, two patients had adenocarcinomas, one patient had a small-cell carcinoma, one patient had a large-cell carcinoma and one patient a non-small-cell carcinoma. Histopathological data were obtained by mediastinoscopy and biopsy. At the time of the PET studies, none of the patients had undergone radiotherapy or chemotherapy. All patients gave written informed consent. PET scanning was performed using a Scanditronix PET PC-4096-15WB with eight detector rings yielding 15 imaging planes (*5*). The imaged volume covered 10.4 cm in the axial direction. The optimum in-plane resolution of the scanner was 4.9 mm in the center of the field of view with an axial resolution of 6 mm (FWHM). Images were reconstructed by filtered backprojection using a Hanning filter with a filter width of 5 mm leading to an in-plane image resolution of 7.1 mm. In order to perform measured attenuation correction, transmission scans were done before tracer injection using a ^{68}Ge rotating pin source. For better visual demonstration, the image in Figure 4 was reconstructed by iterative reconstruction (*6*). In order to ensure optimal repositioning, the position of the intrathoracic tumor was determined by fluoroscopy in the supine position and marked on the patient's thoracic wall prior to PET imaging. About 2 cm below the caudal margin of the tumor, a line was drawn on the patient's thoracic wall on which the lowest of the eight PET rings was positioned by laser beam control. The patients were first studied

Received Jun. 17, 1992; revision accepted Oct. 7, 1992.
For correspondence or reprints contact: Karl-Josef Langen, MD, Institute of Medicine, Research Center Jülich, POB 1913, 5170 Jülich, Germany.

TABLE 1
Plasma Glucose Level, DAR, DARcorr and MR in Bronchial Carcinomas Under Fasting Conditions and During Glucose Infusion

Patient no.	PG (mg/100 ml)		DAR tumor		DARcorr. tumor		MR tumor	
	Fasted	Gluc. Load	Fasted	Gluc. Load	Fasted	Gluc. Load	Fasted	Gluc. Load
1	108.8	154.6	4.79	2.99	5.21	4.62	—	—
2	88.5	130.0	5.91	2.42	5.23	3.15	—	—
3	72.8	169.8	5.41	2.17	3.94	3.68	3.90	5.75
4	81.0	154.0	10.47	5.12	8.48	7.88	9.31	9.77
5	61.8	169.2	5.42	3.89	3.35	6.58	5.11	5.05
6	77.8	192.0	2.65	1.45	2.06	2.78	2.68	2.46
7	112.0	180.0	4.27	3.12	4.78	5.62	5.28	3.98
8	89.0	171.0	2.89	2.38	2.57	4.07	—	—
9	96.0	134.6	5.46	2.70	5.24	3.63	7.12	7.15
10	64.6	155.8	5.67	3.09	3.66	4.81	3.62	4.33
11	67.6	169.4	4.21	2.29	2.85	3.88	2.23	2.45
12	93.4	181.8	3.40	2.36	3.18	4.29	2.55	2.44
13	82.0	224.0	6.42	2.35	5.26	5.26	7.65	6.45
14	91.2	187.0	3.53	1.89	3.22	3.53	1.70	2.07
15	82.8	151.6	5.49	4.38	4.55	6.64	5.41	7.63
mean ± s.d.	84.6 ± 14.7	168.3 ± 23.6	5.07 ± 1.89	2.84 ± 0.97	4.24 ± 1.59	4.70 ± 1.45	4.71 ± 2.38	4.96 ± 2.46
	$p < 0.001$		$p < 0.001$		ns		ns	

PG = plasma glucose level.

after an overnight fast and two days later during intravenous infusion of a 20% glucose solution. The infusion was started 20 min before the injection of FDG, plasma glucose levels were measured every 4 min and glucose infusion was controlled by a computer program so that the plasma glucose level under fasting conditions was nearly doubled. The plasma glucose level was maintained during the entire PET procedure. The mean value of the plasma glucose levels for each patient during the PET studies is given in Table 1.

FDG was synthesized as previously described (*7*) and produced according to a Drug Master File created at the Institute of Radiochemistry in Jülich. A typical production of FDG was more than 5000 mCi in each batch. The quality control of the final product was ensured by control of the chemical purity, radiochemical purity, specific activity, isotinicity, sterility and the amount of endotoxins. The average specific activity was greater than 10.000 Ci/mmol. A bolus of 10 mCi FDG was injected intravenously in every PET study.

Arterialized blood was drawn through a fine gauge intravenous canula inserted in an anticubital vein on the contralateral side. Dynamic PET scans were acquired in 12 patients over 60 min while in three patients only a static scan was acquired 30 to 60 min after injection of FDG. In order to evaluate FDG uptake in the tumor, regions of interest (ROIs) were manually drawn on the tumor area with increased FDG uptake on four adjacent PET images using a background cutoff of 20%. Necrotic tumor areas were avoided. The tumor area ranged from 3.5 to 70.9 cm^2 with a mean value of 30.5 cm^2. The mean tumor uptake was calculated (weighted for the ROI sizes) as the average of the four regions. The same regions were then transferred to the corresponding slices of the PET study during glucose infusion. The DAR was calculated for all tumors according to the following formula:

$$DAR = \frac{\text{tissue concentration (mCi/g)}}{\text{injected dose (mCi)/body weight (g)}}.$$

Additionally, a corrected DAR value (DARcorr.) was calculated by multiplying the DAR by plasma glucose concentration and dividing by 100.

In 12 patients, the metabolic rate of glucose consumption in tumors was calculated with the graphical method introduced by Patlak (*8*) and Gjedde et al. (*9*) using sequential uptake data in the tissue and the plasma input function. The slope of the linear part of this plot represents k1k3/(k2 + k3), where k1, k2 and k3 are the rate constants of the three-compartment model of FDG metabolism. By using this ratio, the metabolic rate for glucose was calculated according to Huang et al. (*10*) by:

$$MR = \frac{Cp}{LC}\frac{k1\ k3}{(k2 + k3)},$$

where Cp is the plasma glucose level and LC is the lumped constant. The lumped constant accounts for the different affinities of glucose and FDG at the blood/tumor interface and the enzyme hexokinase, and was assumed to be constant in the fasted and glucose load study. In this study, a value of 0.654, which has been determined in rat ascites tumors (*11*), was used for all tumors.

RESULTS

The plasma glucose level of the patients increased from 84.6 ± 14.7 mg/100 ml under fasting conditions to 168.3 ± 23.6 mg/100 ml during glucose infusion ($n = 15$, $p < 0.001$, see Table 1). The average DAR value decreased from 5.07 ± 1.89 under fasting conditions to 2.84 ± 0.97

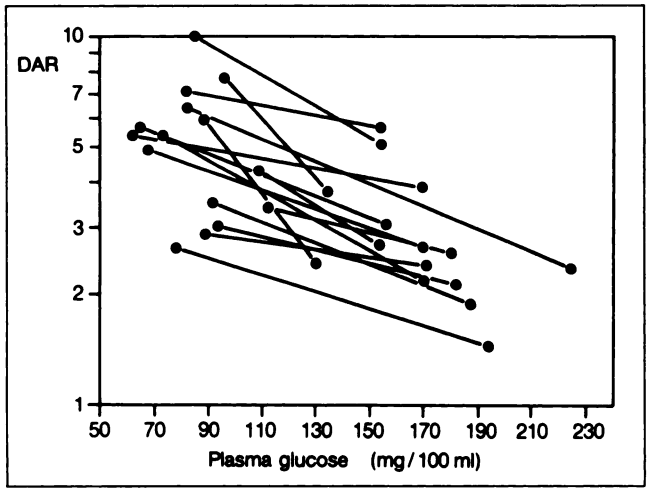

FIGURE 1. Changes of the dose absorption ratio of FDG uptake in bronchial carcinomas under fasting conditions (left) and at elevated plasma glucose levels (right).

(−41.8% ± 15%, n = 15, $p < 0.001$) during glucose infusion. The absolute DAR values of all tumors are plotted in Figure 1. Correction of the DAR by plasma glucose level eliminated significant differences (4.24 ± 1.59 versus 4.70 ± 1.45, n = 15, ns), but there were considerable changes in individual patients (Fig. 2). A PET scan of a large squamous-cell carcinoma in the right lower lobe of the lung is presented in Figure 3. The images are normalized to the same background. It is evident that FDG uptake in the tumor decreases considerably when the plasma glucose level is elevated. At the same time, there is increased FDG uptake in the heart. The MR data in tumors, as determined by the Patlak approach, are given in Figure 4. Although some tumors

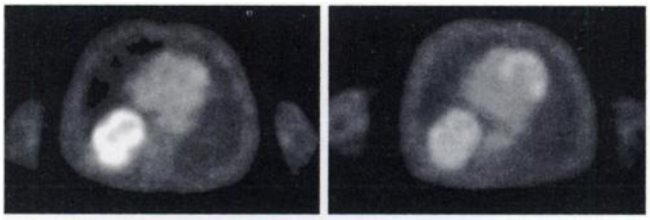

FIGURE 3. FDG uptake in a large squamous-cell carcinoma in the right lower lobe of the lung (left) under fasting conditions and during glucose infusion (right). Images are reconstructed by iterative reconstruction and normalized to the same background. There is considerable decrease in FDG uptake in the tumor at elevated plasma glucose levels.

showed minor changes, the majority remained constant (mean value 4.71 ± 2.38 mg/100 ml/min versus 4.86 ± 2.46 mg/100 ml/min, n = 12, ns).

DISCUSSION

It is well known that 2-deoxyglucose competes with glucose for carrier-mediated transport into the mammalian brain and serves as an alternative substrate for hexokinase (*12,13*). Michaelis-Menten kinetics can be applied to determine the reaction rates of the above hexoses competing for hexokinase and the glucose transporter. The competitive displacement of FDG by plasma glucose depends on the value of the Michaelis-Menten constant K_m of glucose transport and of hexokinase, respectively (*14*).

If the K_m is low in relationship to physiological plasma glucose levels, the reactions are saturated at normal plasma glucose levels. An increase of plasma glucose then leads to a competitive displacement of FDG. If the K_m is high in relationship to physiological plasma glucose levels, the reaction rate increases with glucose concentration so that no competition with FDG is observed.

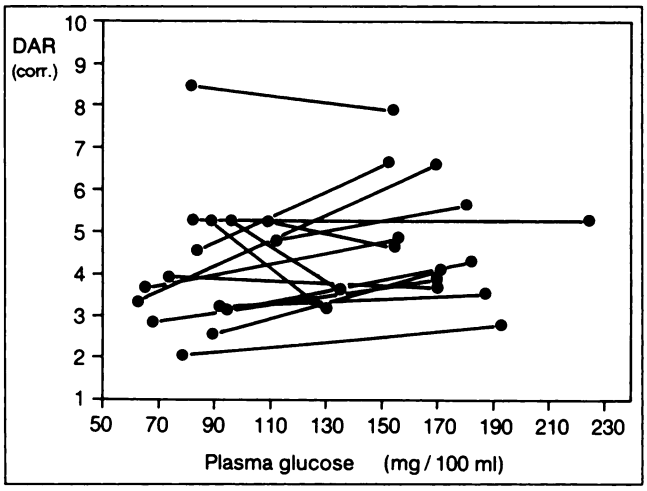

FIGURE 2. Changes of the dose absorption ratio of FDG uptake in bronchial carcinomas corrected by the plasma glucose level under fasting conditions (left) and at elevated plasma glucose levels (right).

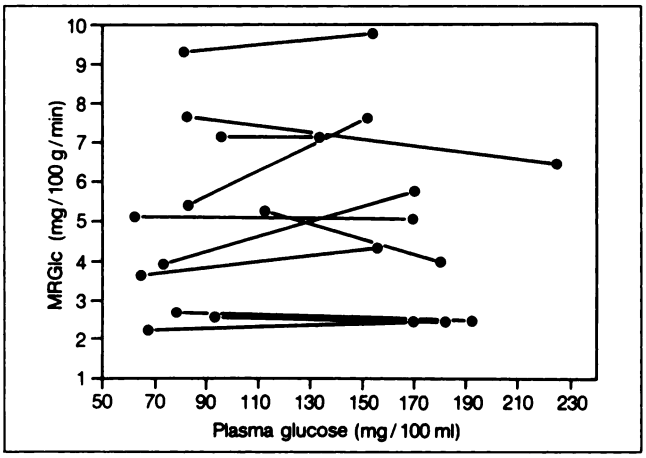

FIGURE 4. Metabolic rate for glucose consumption (MR) in bronchial carcinomas under fasting conditions (left) and at elevated plasma glucose levels (right). The MR appears independent at the plasma glucose level.

The K_m of hexokinase for glucose in normal rat brain has been reported to be 0.067 m*M* (*15*) and corresponds to the "low K_m" hexokinase specifically associated with brain mitochondria (*16*). Compared with normal brain, the hexokinase isolated from intracerebral and subcutaneous gliomas had a higher K_m (0.138 and 0.183 m*M*), indicating a lower affinity for glucose. This may be due to a shift in the isoenzyme pattern of hexokinase type I to type II or III in glioma tissue (*17*). Few data of this kind are available for other human tumors. A study of the effect of glucose loading on FDG uptake in transplantable rat hepatoma showed no correlation between plasma glucose level and FDG uptake, indicating a low affinity K_m in such tumors (*18*). In recent animal experiments with mammary carcinoma, a reduction of FDG uptake after glucose loading was observed (*19*).

This study shows that the DAR of FDG uptake in bronchial carcinomas is influenced greatly by plasma glucose levels, indicating that these tumors have a high affinity for glucose. Although there existed some variation in the degree to which uptake was reduced, all of the tumors, independent of histological type and malignancy grade, showed a decreasing DAR with increasing plasma glucose levels. Although an approach to correct the DAR by the plasma glucose level eliminated the significant difference between fasted and glucose load states, considerable changes of the DARcorr. were observed in individual patients, thus making this approach rather questionable. Therefore, in bronchial carcinomas, variations in the plasma glucose level may make the interpretation of DAR data difficult when used for quantitative comparisons and follow-up studies. The plasma glucose level may be significantly affected during chemo- or glucocorticoid therapy. It remains to be determined whether plasma glucose levels affect the DAR in other human tumors. Competition experiments with other human tumors are needed to clarify this question.

In contrast to the DAR values, the kinetic evaluation of glucose metabolism by the Patlak method yielded more reproducible results. Although reproducibility was high, the absolute values of glucose consumption have to be considered with caution because the lumped constant of the tumors is unknown. While the lumped constant for normal brain tissue has been reported to be 0.52 (*20*), lumped constants for intracerebral gliomas up to 1.17 have been reported (*15*). In the present study, a value of 0.65 for the lumped constant, as determined by direct measurements in rat ascites tumors, was used (*11*). Furthermore, the lumped constant is dependent on plasma glucose levels, ranging in normal brain tissue from 0.42 in hyperglycemia up to 0.67 in hypoglycemia (*21*). In this study, however, no systematic change of glucose metabolic rates in bronchial carcinomas was observed with changing plasma glucose levels, indicating a relatively stable lumped constant in the underlying physiological conditions.

For routine clinical applications, one must keep in mind that quantification of glucose metabolism using the Patlak approach is more time-consuming than the DAR. Dynamic acquisition over a 60-min period as well as plasma samples are needed, making this method more labor-intensive. Thus, nonkinetic measurements have the advantage of simplicity.

In summary, this study demonstrates that the DAR of FDG uptake in bronchial carcinomas is influenced significantly by plasma glucose levels. A correction of the DAR by the plasma glucose level improved reproducibility, but considerable changes in some patients remained. If the DAR is considered for quantification of FDG uptake in bronchial carcinomas, variations of the plasma glucose level have to be taken into account. The kinetic evaluation of glucose metabolism by the Patlak graphical approach appears relatively independent of plasma glucose level, but this approach is more labor-intensive. Where an accurate evaluation of tumor glucose metabolism is needed, such as measuring tumor response to therapy, it is advantageous to adhere to kinetic evaluation.

REFERENCES

1. Som P, Atkins HL, Bandoypadhyay D, et al. A fluorinated glucose analogue, 2-fluoro-2-deoxy-D-glucose (^{18}F): nontoxic tracer for rapid tumor detection. *J Nucl Med* 1980;21:670–675.
2. Warburg O. On the origin of cancer cells. *Science* 1956;123:309–314.
3. Strauss LG, Conti PS. The applications of PET in clinical oncology. *J Nucl Med* 1991;32:632–648.
4. Hawkins RA, Choi Y, Huang S-C, Messa C, Hoh CK, Phelps ME. Editorial: quantitating tumor glucose metabolism with FDG and PET. *J Nucl Med* 1992;33:339–344.
5. Rota Kops E, Herzog H, Schmid A, Holte S, Feinendegen LE. Performance characteristics of an eight-ring whole body PET scanner. *J Comput Assist Tomogr* 1990;14:437–445.
6. Ziemons K, Herzog H, Bosetti P, Feinendegen LE. Iterative image reconstruction with weighted pixel contributions to projection elements [Abstract]. *Eur J Nucl Med* 1992;19:587.
7. Hamacher K, Blessing G, Nebeling B. Computer-aided synthesis (CAS) of no-carrier added 2-[^{18}F]fluoro-2-deoxyglucose: an efficient automated system for the amino polyether-supported nucleophilic fluorination. *Appl J Radiat Isot* 1990;41:49–65.
8. Patlak CS, Blasberg RG, Fenstermacher JD. Graphical evaluation of blood-to-brain transfer constants from multiple-time uptake data. *J Cereb Blood Flow Metab* 1983;3:1–7.
9. Gjedde A. High- and low-affinity transport of D-glucose from blood to brain. *J Neurochem* 1981;36:1463–1471.
10. Huang S-C, Phelps ME, Hoffman EJ, Sideris K, Selin CJ, Kuhl DE. Noninvasive determination of local cerebral metabolic rate of glucose in man. *Am J Physiol* 1980;238:E69–E82.
11. Kato A, Diksic M, Yamamoto YL, Feindel W. Quantification of glucose utilization in an experimental brain tumor model by the deoxyglucose method. *J Cereb Blood Flow Metab* 1985;5:108–114.
12. Bachelard HS. Specific and kinetic properties of monosacharide uptake in guinea pig cerebral-cortex in-vivo. *J Neurochem* 1971;18:213–222.
13. Oldendorf WH. Brain uptake of radio-labeled amino acids, amines and hexoses after arterial injection. *Am J Physiol* 1971;221:1629–1639.
14. Sokoloff L, Reivich M, Kennedy C, et al. The [^{14}C]deoxyglucose method for the measurement of local cerebral glucose utilization: theory, procedure, and normal values in the conscious and anesthetized albino rat. *J Neurochem* 1977;28:897–916.
15. Kapoor RR, Spence AM, Muzi M, Graham MM, Abbott GL, Krohn KA. Determination of the deoxyglucose and glucose phosphorylation ratio and the lumped constant in rat brain and a transplantable rat glioma. *J Neurochem* 1989;53:37–44.

16. Sols A, Salas M, Vinuela E. Induced synthesis of liver glucokinase. In: Weber G, ed, *Advances in enzyme regulation*, volume 2. New York: Pergamon Press; 1964:177–188.
17. Bennett MJ, Timperley WR, Taylor CB, Hill SA. Isozymes of hexokinase in the developing, normal and neoplastic human brain. *Eur J Cancer* 1978;14:189–193.
18. Yamada K, Endo S, Fukuda H, et al. Experimental studies on myocardial glucose metabolism of rats with ^{18}F-2-fluoro-2-deoxy-D-glucose. *Eur J Nucl Med* 1985;10:341–345.
19. Wahl RL, Henry CA, Ethier SP. Serum glucose: effects on tumor and normal tissue accumulation of 2-[F-18]-fluoro-2-deoxy-D-glucose in rodents with mammary carcinoma. *Radiology* 1992;183:643–647.
20. Reivich M, Alani A, Wolf A, et al. Glucose metabolic rate kinetic model parameter determination in humans: the lumped constants and rate constants for [F-18]fluorodeoxyglucose and [^{11}C]deoxy-glucose. *J Cereb Blood Flow Metab* 1985;5:179–192.
21. Schuier, Orzi F, Suda S, et al. Influence of plasma glucose concentration on lumped constant of the deoxy-glucose method: effects of hyper-glycemia in the rat. *J Cereb Blood Flow Metab* 1990;10:765–773.

(continued from page 5A)

FIRST IMPRESSIONS

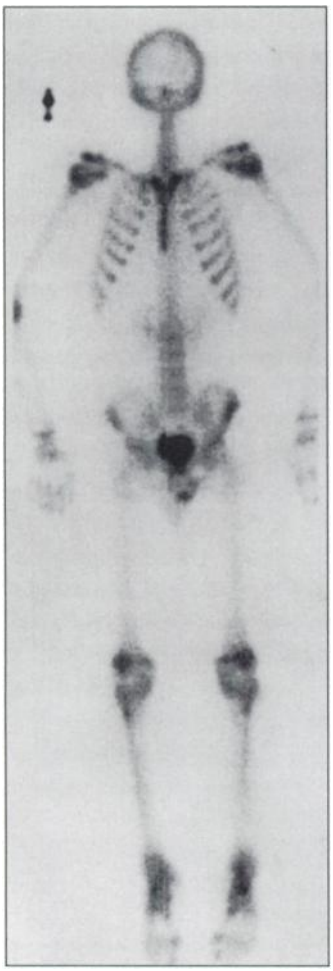

FIGURE 1

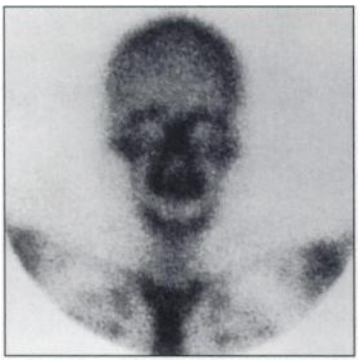

FIGURE 2

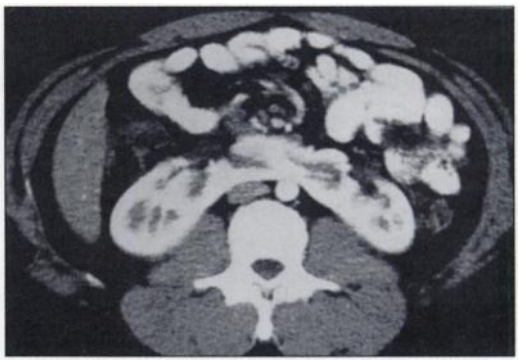

FIGURE 3

PURPOSE
Evaluation of skeletal metastatic potential of an 18-yr-old patient's seminoma. A two-pass gamma camera scan in which the patient positioned his head laterally, first face to left, then face to right, resulted in a superposition image right and left lateral posterior skull (Fig. 2). A horseshoe kidney was incidentally noted and confirmed on a CT scan (Fig. 3).

TRACER
Technetium-99m-MDP, 22 mCi

ROUTE OF ADMINISTRATION
Intravenous

TIME AFTER INJECTION
3.5 hr

INSTRUMENTATION
Siemens 7500 ZLC Bodyscan

CONTRIBUTOR
Robert S. Hattner

INSTITUTION
University of California, San Francisco, California